$y(0)$ under perfect collimation (i.e., $\delta=0$), and should not be a function of energy. (b) The calculated potential $V(x)$ should be independent of the proton energy, $E_p$. This requires that if (a) is satisfied, the angular width of $y(\alpha)$ should be inversely proportional to the square root of energy $E_p$. (c) Measurement of $y(\alpha)$ near $\alpha\approx 0$ produces values of $V(x)$ for $x\lesssim X$. However, values of $V(x)$ near $x=0$ are obtained for large $\alpha$, where the model is not expected to be applicable. Consequently, the estimate of the potential near the center of the channel is not expected to be good.

The experiment was conducted with protons of energies 70 and 100 keV. The beam was swept across the (001) plane of a copper crystal for which the [001] direction was parallel to the surface normal. The plane was crossed at 30° to the surface normal and the stereogram of the (001) surface indicates that no other low-index planes were encountered during the sweep. The data are shown in Fig. 8.

The averaged potential was then calculated using the above equations. The results are shown in Fig. 9. For comparison, the planar-averaged Nielsen potential between two planes may be written

$$V(X)-V(x)=\frac{\pi Z_2 e^2 a_B}{A}K\ln\left[\frac{1-(4x^2/D^2)}{1-(4X^2/D^2)}\right],$$

where $a_B$ is the atomic screening radius and $1/A$ is the atomic density in the plane.[14] This potential is also shown in Fig. 9, where good agreement appears between the calculated and the predicted potential for $x\lesssim X$ (i.e., for $\alpha\approx 0$).

PHYSICAL REVIEW VOLUME 148, NUMBER 1 5 AUGUST 1966

# Wick's Theorem for Spin-½ Operators, with an Application to Spin Waves in Antiferromagnets*†

YUNG-LI WANG, S. SHTRIKMAN,‡ AND HERBERT CALLEN
*Department of Physics, University of Pennsylvania, Philadelphia, Pennsylvania*
(Received 20 December 1965)

An analog of Wick's theorem is developed for spin-½ operators, and a linked diagram expansion for spin Green's functions is derived. As an application we derive the familiar Anderson approximation for spin waves in antiferromagnets, and we then obtain the leading dynamical and kinematical corrections to that approximation. The Oguchi form of correction, usually obtained by a formal expansion in $1/S$ extrapolated to $S=\frac{1}{2}$, is found here as the leading term of an expansion in powers of $1/z$, where $z$ is the number of nearest neighbors. However, the Oguchi result is here found to be valid only for spin waves with wavelengths greater than two or three interspin distances.

## 1. INTRODUCTION

A MAJOR difficulty in the theory of spin systems has been the lack of a practical analog of Wick's theorem. That theorem relates averages of products of many boson or fermion operators to averages of pairs, and it is the basis for the Feynman diagram representation of perturbation theory.[1] In this paper we develop such a theorem for spin operators, albeit of a somewhat more complicated form than in the fermion or boson cases, and we demonstrate the corresponding linked-diagram expansion.

As illustrations of the diagram method for spin operators, we first show that spin excitations in a ferromagnet generate diagrams which can be trivially summed to infinite order, giving the well-known rigorous spin-wave result.

The simplicity of the ferromagnetic case precludes a full demonstration of the diagrammatic method. To illustrate the more general aspects we then consider the nontrivial problem of spin excitations in a Heisenberg antiferromagnet. Summation of the lowest order (simple-chain) diagrams yields the familiar spin-wave approximation of Anderson.[2] We show that if we restrict our attention to spin waves with wavelengths greater than about two interspin distances, the diagrams can be classified according to their order in $1/z$, where $z$ is the number of nearest neighbors. Furthermore this classification is equivalent to a classification according to the order in $\delta S_0^z$, the deviation from perfect alignment in the ground state. The leading diagrams in $1/z$ are chains dressed with bubbles (a dynamical correction) and with loops (a kinematical correction). The resultant correction reproduces the result of Oguchi.[3]

Although the excitation spectrum has been obtained

* Supported by the U. S. Office of Naval Research and the National Science Foundation.
† This work is a contribution of the Laboratory for Research on the Structure of Matter, University of Pennsylvania.
‡ Senior Foreign Scientist Fellow of the National Science Foundation. On leave from the Weizmann Institute of Science, Rehovoth, Israel.
[1] G. C. Wick, Phys. Rev. **80**, 268 (1950). For applications see, for example, S. Schweber, *An Introduction to Relativistic Quantum Field Theory* (Row, Peterson and Company, New York, 1962).
[2] P. W. Anderson, Phys. Rev. **86**, 694 (1952).
[3] T. Oguchi, Phys. Rev. **117**, 117 (1960).

previously, we believe that the present derivation provides a new and instructive perspective to this problem. The Oguchi result nominally follows from an expansion of the Holstein-Primakoff transformation in powers of $1/S$ (keeping only terms of low order). This expansion is a dubious one for $S=\frac{1}{2}$, which is the case here considered. One might conceivably doubt the Oguchi result for this spin value, or one might infer that the nominal expansion in $1/S$ is in fact implicitly coupled to an expansion in some less obvious but more satisfactory parameter. Our calculation indicates that this expansion parameter is $1/z$, but it explicitly limits the result to spin waves of wavelength greater than two or three interspin distances.

In a recent short note Tyablikov and Moskalenko[4] have given an iteration procedure for the decomposition of products of spin-$\frac{1}{2}$ operators. Also, while we were writing the final version of this paper Dr. R. E. Mills called to our attention two short summaries of talks presented at meetings; one by Mills, Kenan, and Korringa[5] at the Congress on Many-Particle Problems in Utrecht, 1960, and one by Kenan[6] at the Eighth International Conference on Low Temperature Physics, 1963. Those authors have clearly developed the same expansion theorem that we subsequently discovered (a full five years later). However, their interest was in thermodynamic properties, and they have given an approximation which appears to be somewhat related to the random-phase variant of Green's-function theories.

## 2. CAUSAL-SPIN GREEN'S FUNCTIONS AND WICK'S THEOREM

We consider a system in which a spin of magnitude $S=\frac{1}{2}$ is localized at each lattice point of a Bravais lattice. The spin operators at the $m$th site are designated by $S_m^+$, $S_m^-$, $S_m^z$. We define the Green's function $G(l,m)$ by

$$G(l,m)=-i(0|P\tilde{S}_l^-(t_l)\tilde{S}_m^+(t_m)|0), \tag{2.1}$$

where $\tilde{S}_l^-(t_l)$ is in the Heisenberg representation (indicated by the tilde); $|0)$ denotes the true ground state; and $P$ is the Dyson time-ordering operator (*not* the usual Wick operator), which arranges operators in order of increasing time from right to left. If an $S^+$ and an $S^-$ operator have equal time arguments the $S^+$ is to be ordered to the left. This definition of the Green's function agrees with the standard definition of causal Green's functions for bosons (for which Dyson and Wick operators are identical). Consequently, the conventional analysis of the spectral representation and analytic properties of the Green's function can be taken over in toto from the familiar boson case.[7] This does *not* imply that the spins are here considered as bosons, for the full spin commutation relations will be retained throughout the analysis.

As usual we now re-express the Green's function in interaction representation. For this purpose we choose some effective field $\omega_l/(g\mu_B)$ to define the unperturbed Hamiltonian; $\omega_l$ will be chosen differently for "up" and "down" spins in the antiferromagnet, but it will be taken as independent of $l$ (the site label) in the ferromagnet. The unperturbed Hamiltonian is

$$\mathcal{H}_0=\sum_l \omega_l S_l^z, \tag{2.2}$$

and the perturbation $\mathcal{H}'$ is

$$\mathcal{H}'=\mathcal{H}-\mathcal{H}_0. \tag{2.3}$$

An operator $O(t)$ in interaction representation is related to the Schrödinger operator $O$ and to the Heisenberg operator $\tilde{O}(t)$ by

$$O(t)=e^{i\mathcal{H}_0 t}Oe^{-i\mathcal{H}_0 t}=\mathcal{S}(t)\tilde{O}(t)\mathcal{S}^{-1}(t), \tag{2.4}$$

where

$$\mathcal{S}(t)=P\exp\left(-i\int_{-\infty}^{t}\mathcal{H}'(t')dt'\right). \tag{2.5}$$

In particular,

$$S_l^{\pm}(t)=e^{\pm i\omega_l t}S_l^{\pm}, \tag{2.6}$$

$$S_l^z(t)=S_l^z=S-S_l^-(t)S_l^+(t)=S-S_l^-S_l^+. \tag{2.7}$$

The unperturbed Green's functions are then

$$G^0(l,m)=-ie^{-i(\omega_l t_l-\omega_m t_m)}\theta(t_l-t_m)\delta_{lm}. \tag{2.8}$$

Furthermore, invoking the usual "adiabatic turning-on theorem" for the effect of the perturbation on the ground state, we obtain in the standard way[7]:

$$G(l,m)=-i\langle 0|PS_l^-(t_l)S_m^+(t_m)\mathcal{S}(\infty)|0\rangle/\langle 0|\mathcal{S}(\infty)|0\rangle, \tag{2.9}$$

where $|0\rangle$ denotes the unperturbed ground state.

The analysis of the Green's function (2.9) will proceed, of course, by series expansion of the operator $\mathcal{S}(\infty)$, Eq. (2.5). We thereby encounter expectation values such as $\langle 0|PS_1^+(t_1)S_2^-(t_2)S_3^+(t_3)\cdots|0\rangle$. In such a product there are, perforce, as many $S^+$ operators as $S^-$ operators (else the product vanishes), and we have taken advantage of the freedom of rearrangement under the $P$ operation to list these in alternating sequence. Because of the separability of the unperturbed density operator such a product factors into similar products each referring to a single site. For a single site the spin-commutation relations for $S=\frac{1}{2}$ are identical to fermion

[4] S. V. Tyablikov and V. A. Moskalenko, Dokl. Akad. Nauk SSSR **158**, 839 (1964) [English transl.: Soviet Phys.—Doklady **9**, 891 (1965)].

[5] R. L. Mills, R. P. Kennan and J. Korringa, Physica **26**, S204 (1960).

[6] R. P. Kenan, in *Low Temperature Physics*, edited by R. O. Davies (Butterworths Scientific Publications, Ltd., London, 1963).

[7] See, for example, A. A. Abrikosov, L. P. Gorkov, and Z. E. Dzyaloshinski, *Methods of Quantum Field Theory in Statistical Physics* (Prentice-Hall, Publishers Inc., Englewood, New Jersey, 1963), Chap. 2.

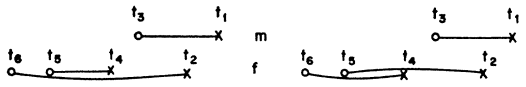


FIG. 1. The two systems of contractions contributing to $\langle 0|PS_f^-(t_6)S_f^+(t_4)S_f^-(t_5)S_f^+(t_2)S_m^-(t_3)S_m^+(t_1)|0\rangle$.

The first contraction carries the signature $(-1)^Q=+1$, and the second contraction carries the signature $(-1)^Q=-1$. Each Green's function line also contributes a factor $(iG^0)$, as indicated in Eq. (2.10). It is assumed in the diagram that $m\neq f$, and that the times are ordered $t_1<t_2<\cdots<t_6$.

commutation relations. These two facts enable us to transcribe the usual fermion form of Wick's theorem, with suitable modifications, to the spin case. A detailed proof is given in Appendix A for the following theorem:

$$\langle 0|PS_f^-(t_f)S_g^+(t_g)S_l^-(t_l)S_m^+(t_m)\cdots|0\rangle = \sum_{\{\alpha\}}\{iG^0(\alpha,\beta)iG^0(\gamma,\delta)\cdots(-1)^Q\}, \quad (2.10)$$

where $\alpha, \beta, \gamma, \delta, \cdots$ is some permutation of the indices $f, g, l, m, \cdots$, and where the summation is over all permutations. The quantity $Q$ is the number of "half-overlapping" pairs of Green's functions in the set $G^0(\alpha,\beta)G^0(\gamma,\delta)\cdots$, defined as follows: We first note that $G^0(\alpha,\beta)$ vanishes unless $\mathbf{r}_\alpha=\mathbf{r}_\beta$, so that each of the nonvanishing Green's functions in the product can be indicated more explicitly as $G^0(\mathbf{r}_\alpha\bar{t}_\alpha,\mathbf{r}_\alpha t_\alpha)$ or $G^0(\mathbf{r}_\gamma\bar{t}_\gamma,\mathbf{r}_\gamma t_\gamma)$, the bar indicating the terminal time. The pair of Green's functions $G^0(\mathbf{r}_\alpha\bar{t}_\alpha,\mathbf{r}_\alpha t_\alpha)$ and $G^0(\mathbf{r}_\gamma\bar{t}_\gamma,\mathbf{r}_\gamma t_\gamma)$ is said to be half-overlapping only if $\mathbf{r}_\alpha=\mathbf{r}_\gamma$ and if either $\bar{t}_\alpha<\bar{t}_\gamma<t_\alpha<t_\gamma$ or $\bar{t}_\gamma<\bar{t}_\alpha<t_\gamma<t_\alpha$. Pictorially, this means that the two Green's functions must be on the same site, the second one starting between the beginning and end of the first one, and surviving it in time.

A pictorial representation of this form of Wick's theorem is particularly useful. Given the product $\langle 0|PS_1^+(t_1)S_2^-(t_2)S_3^+(t_3)\cdots|0\rangle$, we reserve a horizontal line for each different site index in the product, different sites having lines one above another, as in Fig. 1. The horizontal scale denotes time, which proceeds from right to left. Each operator $S_l^+(t_l)$ is represented by a cross on its appropriate site line, at the horizontal distance appropriate to $t_l$. Each $S_m^-(t_m)$ is similarly represented by a circle. The entire product is then represented by all possible ways of drawing directed lines (unperturbed Green's functions) starting at crosses and proceeding horizontally to the left to terminate on circles. In each such set of contractions one and only one Green's function line can terminate on any circle, or initiate on any cross. The sign to be associated with each diagram is $(-1)^Q$, where $Q$ is the number of pairs of half-overlapping Green's-function lines.

To illustrate the applicability of this diagrammatic representation to the series expansion of Green's functions we first consider the admittedly trivial case of spin waves in a Heisenberg ferromagnet.

## 3. THE HEISENBERG FERROMAGNET

The Hamiltonian of the system to be considered is

$$\mathcal{H}=-\sum_{f,g}J_{fg}\mathbf{S}_f\cdot\mathbf{S}_g+\mu H\sum_f S_f^z+E_0, \quad (3.1)$$

where $\mu\equiv g\mu_B$ is the magnetic moment per spin and $H$ is the externally applied magnetic field. $J_{fg}$ is the exchange integral between sites $f$ and $g$. The ground state has all spins down, and $E_0$ is chosen so that the energy of this state is zero:

$$E_0=NJ(0)S^2+\mu HNS, \quad (3.2)$$

where

$$J(0)=\sum_g J_{fg}. \quad (3.3)$$

We choose the unperturbed Hamiltonian as

$$\mathcal{H}_0=\omega_0\sum_f S_f^+S_f^-,$$

with

$$\omega_0=J(0)+\mu H,$$

whence the perturbation Hamiltonian is

$$\mathcal{H}'=-\sum_{f,g}[J_{fg}S_f^+S_g^-+J_{fg}'S_f^+S_f^-S_g^+S_g^-]. \quad (3.4)$$

We here distinguish between the "transverse component" of the exchange $J_{fg}$ and the "longitudinal component" $J_{fg}'$, although these subsequently will be taken as equal.

We now consider the Green's function $G(\bar{l},m)\equiv G(\mathbf{r}_l\bar{t}_l,\mathbf{r}_m t_m)$, noting a notational convention which will prove useful henceforth. That is, the index $\bar{l}$ denotes both the time $\bar{t}_l$ and the spatial index $\mathbf{r}_l$, the bar distinguishing the terminal time, or the time associated with an $S^-$ operator, but not affecting the spatial index.

As in other diagrammatic expansions the numerator of the Green's function $G(\bar{l},m)$ [as given in Eqs. (2.9) and (2.5)] can be expanded in the form

$$\begin{aligned}-i\langle 0|PS_l^-(\bar{t}_l)S_m^+(t_m)\mathcal{S}(\infty)|0\rangle &= -i\langle 0|PS_l^-(\bar{t}_l)S_m^+(t_m)|0\rangle+(-i)^2\\ &\times\int_{-\infty}^{\infty}dt_1\langle 0|PS_l^-(\bar{t}_l)S_m^+(t_m)\mathcal{H}'(t_1)|0\rangle+\frac{(-i)^3}{2!}\\ &\times\int_{-\infty}^{\infty}dt_1\int_{-\infty}^{\infty}dt_2\langle 0|PS_l^-(\bar{t}_l)S_m^+(t_m)\mathcal{H}'(t_1)\mathcal{H}'(t_2)|0\rangle\\ &+\cdots. \quad (3.5)\end{aligned}$$

This series can be represented as follows: One starts with the source point $m$ and the terminal point $\bar{l}$, as in Fig. 2. These are then connected with all possible diagrams involving horizontal Green's-function lines and vertical interaction (wavy) lines. All Green's-function lines must be directed from right to left, and the end point of one must be connected by a vertical wavy line

to the initial point of another, except at the "external points" $\bar{l}$ and $m$. The vertical interaction lines correspond either to transverse or longitudinal interactions, and these are distinguished by their mode of connection to Green's-function lines. Each vertical interaction line of transverse type connects two Green's functions, one terminating and one initiating at the respective ends of the interaction line. Each longitudinal-type interaction line connects four Green's functions, one terminating and one initiating at *each* end of the interaction line. The contribution of such a diagram to $G(\bar{l},m)$ is obtained by associating $-J_{fg}$ with each transverse-type (vertical) interaction line, $-iJ_{fg}'$ with each longitudinal-type (vertical) interaction line, an unperturbed Green's function with each horizontal line, summing over all intermediate lattice sites (vertical positions) and integrating over all intermediate times (horizontal positions). The factor $1/n!$ appearing in Eq. (3.5) need not be considered, for reasons which will be discussed below.

We note the following facts immediately:

1. Since all unperturbed Green's functions must be directed from right to left, the Green's function $G(\bar{l},m)$ vanishes unless the source point $m$ is to the right of the terminal point $\bar{l}$ (i.e., $\bar{t}_l > t_m$).

2. All diagrams proceed monotonically to the left, and therefore no half-overlapping diagrams occur.

3. The longitudinal interaction makes no contribution to any diagram because of 1 and 2 above.

4. There are no unconnected diagrams, or diagrams with parts disjoint from the source and terminal points $m$ and $\bar{l}$.

5. There are no diagrams whatsoever corresponding to the denominator $\langle 0|S(\infty)|0\rangle$ of the Green's function, except for the trivial diagram represented by unity. This reflects the fact that the ground state in the absence of the perturbation is identical to the ground state in the presence of the perturbation, so that $|0\rangle = S(t)|0\rangle$, consequently, taking $t=\infty$,

$$\langle 0|S(\infty)|0\rangle = \langle 0|0\rangle = 1. \tag{3.6}$$

Because of the above considerations we see that Fig. 2 gives the zero-order, first-order, second-order, and third-order diagrams contributing to the Green's function $G(\bar{l},m)$.

We need only concern ourselves now with the factors $1/n!$ appearing in Eq. (3.5), and then proceed to sum the diagrams of Fig. 2. Consider a diagram of $n$th order, having $n$ wavy lines. Each wavy line corresponds to one free time index, over which we must integrate. The labels $t_1, t_2, \cdots, t_n$ of these integration variables may be permuted in $n!$ ways, to give $n!$ equivalent diagrams. If we consider only one such diagram, we need not divide by $n!$. We therefore consider only a single diagram of each structure, two diagrams being said to be of the same structure if one can be distorted continuously into the other, ignoring all internal labels.

Another way of looking at the statement above is to recall that in the derivation[7] of the series expansion for $S(\infty)$, the form given in Eq. (3.5) is a secondary result. The primary result of the standard derivation is similar, except that the $1/n!$ factors are absent, whereas the multiple integrals are of the form $\int_{-\infty}^{\infty} dt_1 \int_{-\infty}^{t_1} dt_2 \int_{-\infty}^{t_2} dt_3 \cdots$ rather than all extending from $-\infty$ to $\infty$. The unperturbed Green's functions insure that our integrals actually are of this form, and the $1/n!$ factors consequently need never arise.

To summarize, then, the Green's function $G(\bar{l},m)$ can be read from Fig. 2 as follows:

---

$$G(\bar{l},m) = G^0(\bar{l},m) + \int_{-\infty}^{+\infty}\int_{-\infty}^{+\infty} dt_l d\bar{t}_m G^0(\bar{l},l)[-J_{lm}\delta(t_l-\bar{t}_m)]G^0(\bar{m},m) + \sum_{r_1}\int_{-\infty}^{+\infty}\cdots\int_{-\infty}^{+\infty} dt_l d\bar{t}_1 dt_1 d\bar{t}_m G^0(\bar{l},l)[-J_{l1}\delta(t_l-\bar{t}_1)]$$
$$\times G^0(1,1)[-J_{1m}\delta(t_1-\bar{t}_m)]G^0(\bar{m},m) + \sum_{r_1,r_2}\int_{-\infty}^{+\infty}\cdots\int_{-\infty}^{+\infty} dt_l d\bar{t}_1 dt_1 d\bar{t}_2 dt_2 d\bar{t}_m G^0(\bar{l},l)[-J_{l2}\delta(t_l-\bar{t}_2)]$$
$$\times G^0(\bar{2},2)[-J_{21}\delta(t_2-\bar{t}_1)]G^0(\bar{1},1)[-J_{1m}\delta(t_1-\bar{t}_m)]G^0(\bar{m},m) + \cdots, \tag{3.7}$$

or, defining $\delta G^{(n)}(\bar{l},m)$ by

$$G(\bar{l},m) = G^0(l,m) + \sum_{n=1}^{\infty}\delta G^{(n)}(\bar{l},m), \tag{3.8}$$

$$\delta G^{(n)}(\bar{l},m) = (-1)^n(-i)^{n+1}\int_{-\infty}^{\infty}\cdots\int_{-\infty}^{\infty} dt_l dt_{n-1}\cdots dt_2 dt_1 e^{-i\omega_0(\bar{t}_l-t_m)}\theta(\bar{t}_l-t_l)\theta(t_l-t_{n-1})\theta(t_{n-1}-t_{n-2})\cdots$$
$$\times\theta(t_2-t_1)\theta(t_1-t_m)\sum_{r_1\cdots r_{n-1}} J_{l,n-1}J_{n-1,n-2}J_{n-2,n-3}\cdots J_{21}J_{1m}, \tag{3.9}$$

$$= -ie^{-i\omega_0(\bar{t}_l-t_m)}\theta(t_l-t_m)\frac{i^n(\bar{t}_l-t_m)^n}{n!}\sum_{r_1\cdots r_{n-1}} J_{l,n-1}\cdots J_{21}J_{1m}. \tag{3.10}$$

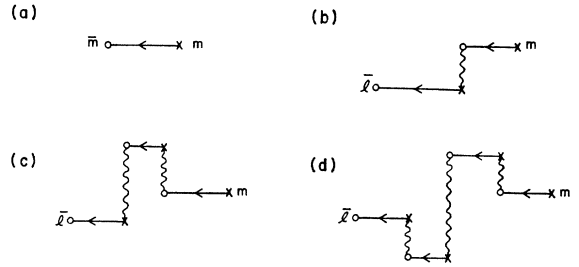


FIG. 2. Zero-order to third-order diagrams for a ferromagnet. The zero-order diagram contributes only if $r_m = r_l$.

It is convenient to simplify this term further by introducing the Fourier components of $J_{ij}$:

$$J_{ij}=\frac{1}{N}\sum_{\mathbf{k}} J(\mathbf{k})\exp[i\mathbf{k}\cdot(\mathbf{r}_i-\mathbf{r}_j)], \tag{3.11}$$

whence

$$\delta G^{(n)}(\bar{l},m)=-ie^{-i\omega_0(\bar{t}_l-t_m)}\theta(\bar{t}_l-t_m)\frac{i^n(\bar{t}_l-t_m)^n}{n!}$$
$$\times\frac{1}{N}\sum_{\mathbf{k}}(J(\mathbf{k}))^n\exp[i\mathbf{k}\cdot(\mathbf{r}_l-\mathbf{r}_m)], \tag{3.12}$$

and

$$G(\bar{l},m)=-i\theta(\bar{t}_l-t_m)$$
$$\times\frac{1}{N}\sum_{\mathbf{k}}\exp\{i[J(\mathbf{k})-\omega_0](\bar{t}_l-t_m)+i\mathbf{k}\cdot(\mathbf{r}_l-\mathbf{r}_m)\}. \tag{3.13}$$

The Fourier component $G(\mathbf{k},\omega)$ in $\mathbf{k}$, $\omega$ space is, then,

$$G(\mathbf{k},\omega)=\frac{1}{\omega-\omega(\mathbf{k})+i\delta}, \tag{3.14}$$

where

$$\omega(\mathbf{k})=\omega_0-J(\mathbf{k})=\mu H+J(0)-J(\mathbf{k}). \tag{3.15}$$

Thus $G(\mathbf{k},\omega)$ has the standard form of an independent-excitation free Green's function, with the energy $\omega(\mathbf{k})$. This energy agrees, of course, with the well-known spin-wave excitation energy.

## 4. THE HEISENBERG ANTIFERROMAGNET

Having illustrated the simplest aspects of the diagram method by consideration of the ferromagnet, we proceed to the nontrivial problem of the Heisenberg antiferromagnet which will exhibit the diagram expansion in much greater generality.

We consider a system of two crystallographically equivalent interpenetrating sublattices such that the nearest neighbors of an ion on one sublattice lie entirely on the other sublattice. Designating the spins on the "down" sublattice by the running index $f$ and those on the "up" sublattice by the index $g$, the Hamiltonian is taken as

$$\mathcal{H}=\mu(H_A+H)\sum_f S_f{}^z-\mu(H_A-H)\sum_g S_g{}^z$$
$$+2\sum_{f,g}J_{fg}\{\tfrac{1}{2}(S_f{}^+S_g{}^-+S_g{}^+S_f{}^-)\}$$
$$+2\sum_{f,g}J_{fg}'S_f{}^zS_g{}^z, \tag{4.1}$$

where $H$ is the external field and $H_A$ is a staggered field which removes ground-state degeneracies, but which can be allowed to approach zero at the end of the calculation (or, alternatively, interpreted as a magnetocrystalline anisotropy).

It is convenient to express $g$-site operators in a coordinate system rotated 180° around the $x$ axis, so that

$$R_g{}^-\equiv S_g{}^+,\quad R_g{}^+\equiv S_g{}^-,\quad R_g{}^z\equiv -S_g{}^z. \tag{4.2}$$

Then the Hamiltonian can be written as the sum of an unperturbed part $\mathcal{H}_0$ and a perturbation $\mathcal{H}'$

$$\mathcal{H}=\mathcal{H}_0+\mathcal{H}', \tag{4.3}$$

$$\mathcal{H}_0=\omega_d\sum_f S_f{}^+S_f{}^-+\omega_u\sum_g R_g{}^+R_g{}^-, \tag{4.4}$$

$$\mathcal{H}'=\sum_{f,g}J_{fg}(S_f{}^+R_g{}^++R_g{}^-S_f{}^-)$$
$$-\sum_{f,g}2J_{fg}'S_f{}^+S_f{}^-R_g{}^+R_g{}^-, \tag{4.5}$$

where

$$\omega_d=\mu(H_A+H)+J'(0), \tag{4.6}$$

$$\omega_u=\mu(H_A-H)+J'(0), \tag{4.7}$$

and

$$J'(0)=\sum_g J_{fg}'=\sum_f J_{fg}'. \tag{4.8}$$

The unperturbed ground state is then defined by

$$S_f{}^-|0\rangle=0,\quad R_g{}^-|0\rangle=0. \tag{4.9}$$

We define two kinds of unperturbed Green's functions

$$G^0(\bar{f}',f)=-i\langle 0|PS_{f'}{}^-(\bar{t}_{f'})S_f{}^+(t_f)|0\rangle$$
$$=-ie^{-i\omega_d(\bar{t}_{f'}-t_f)}\theta(\bar{t}_{f'}-t_f)\delta_{f'f} \tag{4.10}$$

and

$$\mathcal{G}^0(\bar{g}',g)=-i\langle 0|PR_{g'}{}^-(\bar{t}_{g'})R_g{}^+(t_g)|0\rangle$$
$$=-ie^{-i\omega_u(\bar{t}_{g'}-t_g)}\theta(\bar{t}_{g'}-t_g)\delta_{g'g}. \tag{4.11}$$

Henceforth the indices in a $G^0$ function will be understood to apply to the down sublattice, whether they are labelled by $f$ or by some other convenient running index, and similarly for $\mathcal{G}^0$.

In contrast to the ferromagnetic case, the linked-diagram expansion theorem for the Green's function $G(\bar{l},m)$ [Eq. (2.9)] is no longer trivial, for the denominator now generates diagrams which cancel the unlinked diagrams in the numerator. Before demonstrating this cancellation we consider the numerator of $G(\bar{l},m)$, ex-

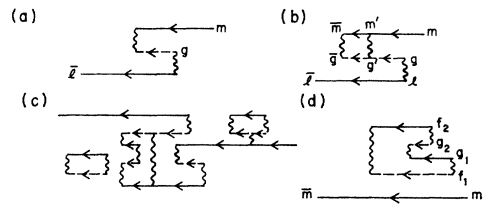

FIG. 3. Representative diagrams in the series expansion of the numerator of the Green's function.

panding it in terms of unperturbed Green's functions by Wick's theorem. The resultant series can be represented as follows. We start with the source point $m$ and the terminal point $\bar{l}$, as in Fig. 3. We then draw all possible diagrams involving horizontal Green's function lines and vertical interaction (wavy) lines. There are two types of Green's function lines; solid lines to represent $f$-site functions ($G^0$'s) and dotted lines to represent $g$-site functions ($\mathcal{G}^0$'s). Each must be directed from right to left. There are two types of interaction lines. A transverse-type of interaction line vertically connects the initial point of a $G^0$ line to the initial point of a $\mathcal{G}^0$ line, or a terminal point of a $G^0$ line to the terminal point of a $\mathcal{G}^0$ line. A longitudinal type of interaction line vertically connects four Green's functions, with a $G^0$ initial and a $G^0$ terminal point at one end, and a $\mathcal{G}^0$ initial and a $\mathcal{G}^0$ terminal point at the other end. Both disconnected and connected diagrams must be considered.

The contribution of a diagram is obtained as in the ferromagnet. Each solid horizontal line represents a $G^0$, each dotted line a $\mathcal{G}^0$, each transverse type of interaction line represents $(+J_{fg})$, and each longitudinal type of interaction line represents $(-2iJ_{fg}')$. Again we must sum over all internal sites and integrate over all internal times, with appropriate parities assigned. The parity of the diagram is determined by the number of half-overlapping pairs of unperturbed Green's functions, and the parity changes in a complicated fashion as one integrates over the internal times (a problem to which we return in the next section). Finally we must divide the contribution of each diagram by a symmetry factor $\gamma$. This symmetry factor is equal to the number of ways in which the diagram can be rotated or reflected into itself; an example in which $\gamma=2$ is shown in Fig. 3(d). The symmetry factor $\gamma$ is discussed in various standard references,[8] and the manner in which it arises in our problem is discussed in Appendix B.

Although the above convention for the diagrammatic expansion of the numerator of $G(\bar{l},m)$ is formally correct, it is far from practical. The difficulty arises from the complicated behavior of the parity factor $(-1)^Q$ as the time integrations are carried out. The essence of our theory lies in a method of coping with this complication, to which we now turn our attention.

[8] For example, J. Hubbard, Proc. Roy. Soc. (London) **A240**, 539 (1957).

## 5. THE "LOCK-DIAGRAM" CONVENTION, AND THE LINKED-DIAGRAM THEOREM

To eliminate the parity changes which occur as Green's function lines overlap, wholly or partially, we introduce a new diagram convention.

Consider the diagram of Fig. 4(a). If $\bar{t}_f<t_{f'}$, as shown, the parity of the diagram is positive. It becomes negative when $t_f<t_{f'}<\bar{t}_f<\bar{t}_{f'}$, or when $t_{f'}<t_f<\bar{t}_{f'}<\bar{t}_f$. We replace this "old-type" diagram by the sum of "new-type" diagrams, shown in Fig. 4 (b), (c), and (d). In Fig. 4(b) the parity of the diagram is to be interpreted as positive, independent of the overlapping or non-overlapping of the Green's-function lines during integration. Figure 4(c) and Fig. 4(d) are then the correction diagrams. Each has a weight of $-2$, and the encirclement of the two half-overlapping lines indicates that the ranges of time integrations are to be limited so that the Green's functions remain half-overlapping. These two Green's-function lines are said to be "locked" in the correction diagram. Similarly Fig. 4(e) is replaced by Fig. 4 (f), (g), and (h).

All accidental half-overlaps henceforth are to be ignored in the contributions of "main diagrams." Correction diagrams contain one or more "locks," limiting the range of integration of internal time variables (and of summation of internal site indices). The weight of such a correction diagram is $(-2)^L$, where $L$ is the number of locks.

To corroborate that $(-2)^L$ is the proper weight of the correction diagram, consider the situation in which there are $L$ pairs of half-overlapping Green's functions (more than one pair can share a common unperturbed Green's function). The parity of the diagram should be $(-1)^L$, rather than the value $(+1)$ assigned in the main diagram. In addition to appearing as an accidental overlap in the main diagram, the diagram has also appeared as an accidental overlap in each of the $\binom{L}{1}$ diagrams with a single lock. Similarly, it has appeared in each of the $\binom{L}{2}$ correction diagrams with 2 of the $L$ pairs locked, etc. If we associate the factor $(-2)$ with

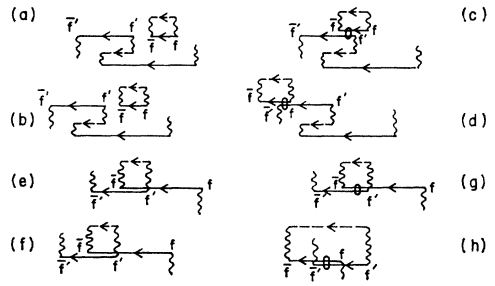

FIG. 4. Replacement of "old-type" diagrams by "main" diagrams plus "lock" diagrams. The old-type diagram (a) is replaced by the new-type "main diagram" (b) and the two correction diagrams (c) and (d). Also the old-type diagram (e) is replaced by the main diagram (f) and the two correction diagrams (g) and (h).

each locked half-overlapping pair, the total weight associated with the case of $L$ overlaps will then be

$$1+(-2)\binom{L}{1}+(-2)^2\binom{L}{2}+\cdots+(-2)^L\binom{L}{L}=(-1)^L, \quad (5.1)$$

which is correct.

The final aspect of the diagram method, which remains to be proved, is the cancellation of unlinked diagrams in the numerator and denominator of $G(\bar{l},m)$.[9] The denominator $\langle 0|\mathcal{S}(\infty)|0\rangle$ is represented by closed loop diagrams with no external points. The numerator generates linked diagrams with external points and also unlinked diagrams. Each such unlinked diagram is a product of the contributions of its linked and its disjoint parts. Collecting all diagrams with a common externally connected portion, their disjoint portions reproduce the denominator. These cancel, and finally only connected diagrams need be considered. That is

$$G(\bar{l},m)=-i\langle 0|PS_l^-(\bar{t}_l)S_m^+(t_m)\mathcal{S}(\infty)|0\rangle_{\text{connected diagrams}} \quad (5.2)$$

It must be noted that a lock can connect an otherwise-unconnected diagram. Thus the diagram of Fig. 4(c) is connected.

## 6. SIMPLE SPIN WAVES; SUMMATION OF CHAIN DIAGRAMS

Before considering the relative importance of the various types of diagrams we shall simply (and arbitrarily) proceed to sum all diagrams which contain neither locks nor longitudinal interactions, that is, the simple "chain" diagrams shown in Fig. 5. We shall find that these diagrams lead to the familiar simple spin-wave theory first given by Anderson.[2] These then provide a zero-order theory, to be corrected by the addition of those diagrams with locks and longitudinal interactions. The classification of the correction diagrams according to their order in $1/z$ (where $z$ is the number of nearest neighbors) will be developed and discussed in Sec. 8.

The summation of diagrams in the antiferromagnet is complicated by the interdependence of the ranges of integration of the free internal time indices. For example, in the fourth-order diagram of Fig. 5(b) the upper limit of integration of $t_g(=t_f)$ is either $\bar{t}_f$ or $\bar{t}_g$, depending on which of these is the earlier. As the order of the diagram increases, the conditions which determine the ranges of integration rapidly escalate in complexity. Fortunately, however, in the Fourier-transformed representation of the diagrams the restrictions on the integration ranges translates simply into energy-conservation conditions, and the diagrams are then easily summed.

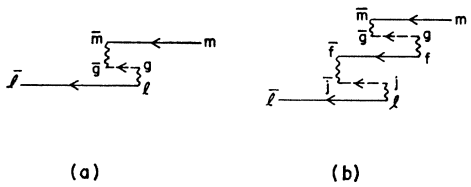


FIG. 5. Chain diagrams.

We first recall that the Green's function $G^0(\bar{f},f)$ is independent of $\mathbf{r}_f$, and its spatial Fourier transform is independent of $\mathbf{k}$. Its temporal transform is

$$G^0(\omega)=\int d(\bar{t}_f-t_f)G^0(\bar{f},f)e^{i\omega(\bar{t}_f-t_f)}=1/(\omega-\omega_d+i\delta)\,, \quad (6.1)$$

and similarly,

$$\mathcal{G}^0(\omega)=1/(\omega-\omega_u+i\delta)\,. \quad (6.2)$$

Consider, as a typical example, the fourth-order chain diagram of Fig. 5. Its contribution is

$$\delta G^{(4)}(\bar{l},m)=\sum_{f,g,j}\int dt_l d\bar{t}_j d\bar{t}_j d\bar{t}_f dt_f dt_g d\bar{t}_g d\bar{t}_m G^0(\bar{m},m)\times J_{mg}\delta(\bar{t}_m-\bar{t}_g)\mathcal{G}^0(\bar{g},g)J_{fg}\delta(t_f-t_g)G^0(\bar{f},f)\times J_{fj}\delta(\bar{t}_f-\bar{t}_j)\mathcal{G}^0(\bar{j},j)J_{jl}\delta(t_j-t_l)G^0(\bar{l},l)\,. \quad (6.3)$$

Taking its Fourier transform we find immediately

$$\delta G^{(4)}(\omega,\mathbf{k})=[G^0(\omega)]^3[\mathcal{G}^0(-\omega)]^2[J(\mathbf{k})]^4. \quad (6.4)$$

This is an example of the general rule that each of the diagrams of Fig. 5 can be re-interpreted in Fourier space, associating an $\omega$ and a $\mathbf{k}$ with each line. Both $\omega$ and $\mathbf{k}$ must be conserved throughout the diagram. Each solid horizontal line carries a contribution of $G^0(\omega)$, each dotted line $\mathcal{G}^0(\omega)$, and each transverse-type interaction line $J(\mathbf{k})$.

The sum of all chain diagrams, $G^c(\omega,\mathbf{k})$ is, then,

$$\begin{aligned}G^c(\omega,\mathbf{k})&=G^0(\omega)+G^0(\omega)\{J(\mathbf{k})\mathcal{G}^0(-\omega)J(\mathbf{k})G^0(\omega)\}\\&\quad+G^0(\omega)\{J(\mathbf{k})\mathcal{G}^0(-\omega)J(\mathbf{k})G^0(\omega)\}^2+\cdots,\\&=G^0(\omega)/[1-J^2(\mathbf{k})\mathcal{G}^0(-\omega)G^0(\omega)]\\&=1/\{[G^0(\omega)]^{-1}-\mathcal{G}^0(-\omega)J^2(\mathbf{k})\}\,, \quad (6.5)\end{aligned}$$

which is of a familiar form, identifying $J^2(\mathbf{k})\mathcal{G}^0(-\omega)$ as the "proper self-energy."

Inserting the values of $G^0(\omega)$ and $\mathcal{G}^0(-\omega)$ from Eqs. (6.1) and (6.2), and taking $J_{fg}'=J_{fg}$,

$$G^c(\omega,\mathbf{k})=A/[\omega-\omega_1(\mathbf{k})+i\delta_1^+]+B/[\omega+\omega_2(\mathbf{k})-i\delta_2^+], \quad (6.6)$$

[9] The linked cluster theorem for fermion and boson systems was first proved by J. Goldstone, Proc. Roy. Soc. (London) **A239**, 267 (1957).

where

$$\omega_1(\mathbf{k})=\tfrac{1}{2}(\omega_d-\omega_u)+[((\omega_d+\omega_u)/2)^2-J^2(\mathbf{k})]^{1/2}$$
$$=\mu H+J(0)((1+\alpha)^2-\gamma_k^2)^{1/2}, \quad (6.7)$$

$$\omega_2(\mathbf{k})=\tfrac{1}{2}(\omega_u-\omega_d)+[((\omega_d+\omega_u)/2)^2-J^2(\mathbf{k})]^{1/2}$$
$$=-\mu H+J(0)((1+\alpha)^2-\gamma_k^2)^{1/2}, \quad (6.8)$$

$$A=\frac{\omega_1(\mathbf{k})+\omega_u}{\omega_1(\mathbf{k})+\omega_2(\mathbf{k})}=\frac{1}{2}\left[1+\frac{1+\alpha}{((1+\alpha)^2-\gamma_k^2)^{1/2}}\right], \quad (6.9)$$

$$B=\frac{\omega_2(\mathbf{k})-\omega_u}{\omega_1(\mathbf{k})+\omega_2(\mathbf{k})}=\frac{1}{2}\left[1-\frac{1+\alpha}{((1+\alpha)^2-\gamma_k^2)^{1/2}}\right], \quad (6.10)$$

$$\alpha=\mu H_A/J(0). \quad (6.11)$$

Thus the excitation energies lie on two branches [with frequencies $\omega_1(\mathbf{k})$ and $\omega_2(\mathbf{k})$] which become degenerate for $H=0$.

For future reference we note that if $\alpha=0$, and if $\omega_d=\omega_u\equiv\omega_0$ (corresponding to $H=0$), then

$$\epsilon(\mathbf{k})\equiv\omega_1(\mathbf{k})=\omega_2(\mathbf{k})=J(0)(1-\gamma_k^2)^{1/2}$$
$$=\omega_0(1-\gamma_k^2)^{1/2}, \quad (6.12)$$

and

$$G^c(\omega,\mathbf{k})=\frac{\omega+\omega_0}{(\omega-\epsilon(\mathbf{k})+i\delta_1^+)(\omega+\epsilon(\mathbf{k})-i\delta_2^+)}. \quad (6.13)$$

Similarly,

$$\mathcal{G}^c(-\omega,-\mathbf{k})=\frac{-\omega+\omega_0}{(\omega+\epsilon(\mathbf{k})-i\delta_1^+)(\omega-\epsilon(\mathbf{k})+i\delta_2^+)}. \quad (6.14)$$

The sublattice magnetization at zero temperature can be obtained easily by noting that

$$(0|S_f^z|0)=-\tfrac{1}{2}+(0|S_f^+S_f^-|0)=-\tfrac{1}{2}+i\lim_{t_f\to\bar{t}_f+}\frac{1}{2\pi N}$$
$$\times\sum_{\mathbf{k}}\int d\omega G(\omega,\mathbf{k})e^{-i\omega(\bar{t}_f-t_f)}. \quad (6.15)$$

Inserting $G^c(\omega,\mathbf{k})$ from Eq. (6.6) and closing the $\omega$ contour in the upper half-plane we pick up the residue of the pole at $\omega=-\omega_2(\mathbf{k})+i\delta_2^+$. Consequently

$$(0|S^z|0)=-\tfrac{1}{2}+\frac{1}{2N}\sum_{\mathbf{k}}\left[\frac{1+\alpha}{((1+\alpha)^2-\gamma_k^2)^{1/2}}-1\right]$$
$$\equiv-\tfrac{1}{2}+\delta S_0^z. \quad (6.16)$$

The results for the spectrum and for the spin deviation $\delta S_0^z$ are recognized to be precisely the simple spin-wave results first found by Anderson.[2]

## 7. THE FIRST-ORDER CORRECTION; LOOP AND BUBBLE DIAGRAMS

Again, at this point, the canonical procedure would dictate that we estimate the magnitude of all types of correction diagrams, demonstrating their classification according to powers of a small expansion parameter $(1/z)$. But again we shall postpone the classification, simply asserting that the dominant correction consists of a particular set of diagrams, to be described and summed below. In Sec. 8, with these first-order corrections in hand, we shall be able to justify our classification *a posteriori*. In addition we will then be able to interpret the diagram series in a more transparent and physical context than would be possible at this juncture.

We claim, then, that if the primary chain diagrams of interest are those with small $\mathbf{k}$, then the dominant correction diagrams are all those with either a single lock, or a single longitudinal interaction. We proceed to sum all such diagrams. More precisely, we shall sum all diagrams such that the irreducible self-energy contains either a single lock or a single longitudinal interaction.

Portions of a diagram containing a single lock are shown in the first two columns of Fig. 6 and portions of a diagram containing a single longitudinal interaction are shown in Fig. 7. These are the twelve basic elements which must be summed.

Our summation procedure can be summarized as follows. We shall show that diagrams (a) and (b) of Fig. 6 can be paired to give a single new loop diagram $(\sigma_1)$, as shown in the Figure. Similarly with (c) and (d), etc. This reduces the number of first-order diagrams to eight. Then $\Sigma_1$ and $\Sigma_3$ (which are the loop and the bubble alone, as shown in Fig. 8) can be considered as self-energy corrections to renormalize $G^0$. Similarly $\Sigma_1'$ and $\Sigma_3'$ (Fig. 8) renormalize $\mathcal{G}^0$. And finally $\Sigma_2$ and $\Sigma_4$ renormalize exchange interactions connecting terminal points of Green's functions, whereas $\Sigma_2'$ and $\Sigma_4'$ renormalize exchange interactions connecting initial points of Green's functions, as shown in Fig. 8.

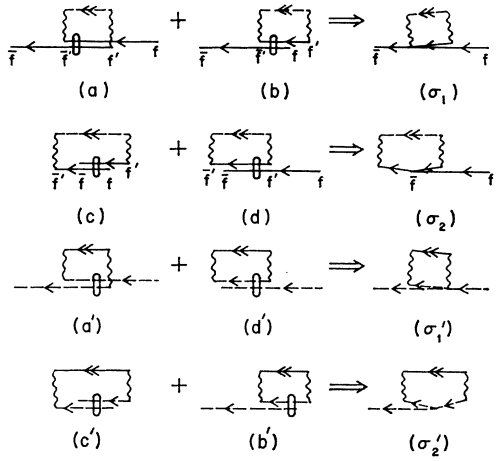


FIG. 6. Pairing of lock diagrams.

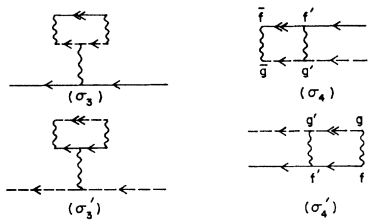

FIG. 7. Longitudinal correction diagrams.

To undertake the program above we first establish the relationships indicated in Fig. 6, in which two basic types of lock diagrams are combined to give a new type of loop diagram. We consider explicitly the combination of Fig. 6(a) and (b) to give the new diagram $(\sigma_1)$.

The sum of the diagram elements (a) and (b) of Fig. 6 is (suppressing the site indices $f$ and $g$)

$$[a+b]=(-2)\int_t^i d\bar{t}_1\int_t^{\bar{t}_1} dt_1 G^0(\bar{t}_1,t)G^0(\bar{t},t_1)\mathcal{G}^0(\bar{t}_1,t_1)$$
$$\times\sum_g J_{fg}^2+(-2)\int_t^i d\bar{t}_1\int_{-\infty}^{t} dt_1 G^0(\bar{t}_1,t_1)$$
$$\times G^0(\bar{t},t)\mathcal{G}^0(\bar{t}_1,t_1)\sum_g J_{fg}^2. \quad (7.1)$$

Inserting the values of the $G^0$'s and $\mathcal{G}^0$, we find the integrands to be identical, so that

$$[a+b]=(-2)\int_t^i d\bar{t}_1\int_{-\infty}^{\bar{t}_1} dt_1 G^0(\bar{t}_1,t_1)$$
$$\times G^0(\bar{t},t)\mathcal{G}^0(\bar{t}_1,t_1)\sum_g J_{fg}^2. \quad (7.2)$$

In this equation we can replace

$$G^0(\bar{t},t)=iG^0(\bar{t},\bar{t}_1)G^0(\bar{t}_1,t), \quad (7.3)$$

in which case we recognize Eq. (7.2) to be precisely the representation of the diagram $(\sigma_1)$ of Fig. 6, providing we adopt the following convention. *The "triple point"* (the point of union of the loop to its parent Green's function) *is to be associated with the factor* $(-2i)$. Similarly the other relations of Fig. 6 can be corroborated directly.

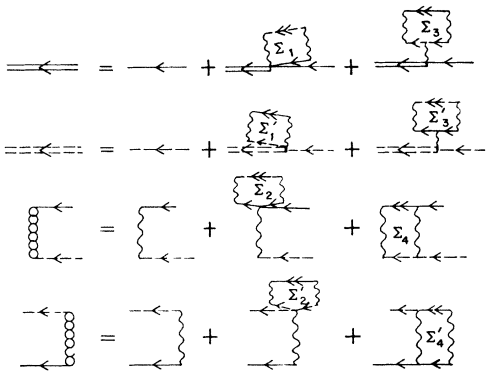

FIG. 8. Renormalization of Green's functions and interaction lines.

Although the loops and bubbles in $(\sigma_1)$, $(\sigma_2)$, $(\sigma_1')$, $(\sigma_2')$, $(\sigma_3)$ and $(\sigma_3')$ have been drawn with only one $f$ site and one $g$ site (and two transverse interactions), it is clear that the loops and bubbles can be of any size. This is accomplished simply by reinterpreting one of the unperturbed Green's functions internal to the loop or bubble as a simple chain Green's function. It should be noted that we are free to so reinterpret either the internal $f$-site Green's function, or the internal $g$-site Green's function; to do both would clearly overcount the diagrams. Henceforth we shall interpret the diagrams in this way, and we have indicated the chain Green's functions by a double arrow in Figs. 6, 7, and 8.

The question of the symmetry factor $\gamma$ of diagrams (b) and (c) of Fig. 6 now arises. The main diagrams, to which (b) and (c) represent corrections, have symmetry factor $\gamma=m$ if the order of the disjoint portion of the diagram is of order $2m$ (cf., Fig. 9). Consequently the same multiplicity factor must be associated with the


FIG. 9. Alternative lockings, which compensate the symmetry factor $\gamma$.

correction diagrams (b) and (d) of Fig. 6. For instance, we should divide the contribution of diagram (a) of Fig. 9 by $\gamma=2$. However, $G^0(\bar{f},f)$ may be locked with another Green's function line in the disjoint diagram, as shown in Fig. 9(b). As both contributions are clearly identical, we regain a factor of 2, which cancels the symmetry factor. Consequently, the symmetry factors do not enter, and the relationships such as $a+b=\sigma_1$ of Fig. 6 remain true for loops of arbitrary size.

The actual summation of the diagrams, indicated schematically in Fig. 8, is most conveniently carried out in the Fourier-transformed space.

Each diagram can be interpreted directly in Fourier space, by the following conventions (which can be corroborated easily in particular cases).

To each directed line there is to be associated an $\omega$ and a $\mathbf{k}$ in such a way that $\omega$ and $\mathbf{k}$ are conserved at each vertex. The contribution of a transverse interaction line is $+J(\mathbf{k})$, independent of its associated $\omega$. The contribution of a longitudinal interaction line is $-2iJ(\mathbf{k})$. A solid line contributes $G^0(\omega)$ or, if it carries a double arrow, $G^c(\omega,\mathbf{k})$. Similarly a dotted line contributes $\mathcal{G}^0(\omega)$ or $\mathcal{G}^c(\omega,\mathbf{k})$. And finally a triple point, connecting a correction loop to its parent diagram, contributes a factor $(-2i)$. Finally all free $\mathbf{k}$'s or $\omega$'s are to be summed or integrated.

Consider now the renormalization of $G^0(\omega)$ by loops and bubbles, as shown in Fig. 8. And, for simplicity, let both external field and anisotropy be zero. A similar analysis can be applied in the presence of these fields, giving a final result also identical to that obtained by Oguchi.[3]

The contribution of the loop is

$$\Sigma_1=(-2i)\frac{1}{N}\sum_{\mathbf{k}}\int\frac{d\omega}{2\pi}G^c(\omega,\mathbf{k})\mathcal{G}^0(-\omega)J^2(\mathbf{k})$$

$$=(-2i)\frac{1}{N}\sum\int\frac{d\omega}{2\pi}\frac{\omega+\omega_0}{(\omega-\epsilon(\mathbf{k})+i\delta_1^+)(\omega+\epsilon(\mathbf{k})-i\delta_2^+)}\times\frac{1}{-\omega-\omega_0+i\delta}J^2(\mathbf{k})$$

$$=\frac{1}{N}\sum_{\mathbf{k}}\frac{J^2(\mathbf{k})}{\epsilon(\mathbf{k})}$$

$$=\frac{1}{N}\sum_{\mathbf{k}}\left[\frac{\omega_0^2}{\epsilon(\mathbf{k})}-\epsilon(\mathbf{k})\right]. \tag{7.4}$$

Recalling that the spin deviation at zero temperature, anisotropy and field is, in the chain approximation [Eq. (6.16)],

$$\delta S_0{}^z=\frac{1}{2N}\sum_{\mathbf{k}}\left[\frac{\omega_0}{\epsilon(\mathbf{k})}-1\right]=\frac{1}{2N}\sum_{\mathbf{k}}\left[\frac{1}{(1-\gamma_{\mathbf{k}}{}^2)^{1/2}}-1\right]; \tag{7.5}$$

and defining

$$\Delta\equiv 1-\frac{1}{\omega_0 N}\sum_{\mathbf{k}}\epsilon(\mathbf{k})=\frac{1}{N}\sum_{\mathbf{k}}[1-(1-\gamma_{\mathbf{k}}{}^2)^{1/2}], \tag{7.6}$$

we have

$$\Sigma_1=\omega_0[2\delta S_0{}^z+\Delta]. \tag{7.7}$$

Similarly the contribution of the bubble is

$$\Sigma_3=[-2iJ(0)]\frac{1}{N}\times\sum_{\mathbf{k}}\int\frac{d\omega}{2\pi}\mathcal{G}^0(-\omega)\mathcal{G}^0(-\omega)G^c(\omega,\mathbf{k})J^2(\mathbf{k}) \tag{7.8}$$

$$=\frac{\omega_0}{N}\sum_{\mathbf{k}}\left[1-\frac{\omega_0}{\epsilon(\mathbf{k})}\right]=-2\omega_0\delta S_0{}^z. \tag{7.9}$$

The Dyson equation corresponding to Fig. 8 is

$$\tilde{G}^0(\omega)=G^0(\omega)+G^0(\omega)[\Sigma_1+\Sigma_3]\tilde{G}^0(\omega), \tag{7.10}$$

or

$$\tilde{G}^0(\omega)=\frac{1}{[G^0(\omega)]^{-1}-\omega_0\Delta}=\frac{1}{\omega-(1+\Delta)\omega_0+i\delta}. \tag{7.11}$$

Similarly, we find

$$\tilde{\mathcal{G}}^0(\omega)=\frac{1}{[\mathcal{G}^0(\omega)]^{-1}-[\Sigma_1'+\Sigma_3']}=\frac{1}{\omega-(1+\Delta)\omega_0+i\delta}. \tag{7.12}$$

Thus renormalization of the unperturbed Green's functions by loops and bubbles merely shifts their poles from $\omega_0$ to $(1+\Delta)\omega_0$.

Consider now the renormalization of a transverse interaction line by the terminal loops $\Sigma_2$ and longitudinal interactions $\Sigma_4$, as in the third relation shown in Fig. 8.

The contribution of the terminal loop $\Sigma_2$ is

$$\Sigma_2=(-2i)\frac{1}{N}\sum_{k}\int\frac{d\omega}{2\pi}G^0(\omega)G^0(\omega)\mathcal{G}^c(-\omega,-\mathbf{k})J^2(\mathbf{k})=\frac{\Sigma_3}{\omega_0}=-2\delta S_0{}^z. \tag{7.13}$$

The diagram segment between $f'$ and $g'$ in $(\sigma_4)$ of Fig. 7 is (assuming the input momentum is $\mathbf{k}$)

$$-2i\frac{1}{N}\sum_{k}\int\frac{d\omega'}{2\pi}G^c(\omega')\mathcal{G}^0(-\omega')\times J(\boldsymbol{k})J(\mathbf{k}-\boldsymbol{k})=J(\mathbf{k})\Sigma_4, \tag{7.14}$$

where

$$\Sigma_4=\frac{1}{N\omega_0}\sum_{\mathbf{k}}\left[\frac{\omega_0^2}{\epsilon(\mathbf{k})}-\epsilon(\mathbf{k})\right]=\frac{\Sigma_1}{\omega_0}=2\delta S_0{}^z+\Delta, \tag{7.15}$$

and where we have used the relationship

$$\sum_{k}f(\boldsymbol{k})J(\boldsymbol{k})J(\mathbf{k}-\boldsymbol{k})=\frac{J(\mathbf{k})}{\omega_0}\sum_{k}J^2(\boldsymbol{k})f(\boldsymbol{k}), \tag{7.16}$$

which holds for all $f(\mathbf{k})$ having the point group symmetry of the crystal.

The renormalization shown schematically in the third relation in Fig. 8 is, then,

$$\tilde{J}(\mathbf{k})=J(\mathbf{k})+\Sigma_2J(\mathbf{k})+\Sigma_4J(\mathbf{k})=J(\mathbf{k})(1+\Delta), \tag{7.17}$$

and the same relation is found for the last renormalization indicated in Fig. 8.

According to the above renormalizations we sum all first-order diagrams by reinterpreting the simple chain diagrams, replacing all Green's-function lines and all interactions by their renormalized counterparts.

Denoting the corresponding approximation to $G(\omega,\mathbf{k})$ by $G^{(1)}(\omega,\mathbf{k})$, we have [analogous to Eq. (6.5)],

$$G^{(1)}(\omega,\mathbf{k})=\frac{1}{[\tilde{G}^0(\omega)]^{-1}-\tilde{\mathcal{G}}^0(-\omega)\tilde{J}^2(\mathbf{k})}, \tag{7.18}$$

$$G^{(1)}(\omega,\mathbf{k})=\frac{\omega+(1+\Delta)\omega_0}{\omega^2-(1+\Delta)^2\omega_0{}^2+(1+\Delta)^2J^2(\mathbf{k})}. \tag{7.19}$$

The spin-wave energies are again degenerate, with

$$\epsilon^{(1)}(\mathbf{k}) = (1+\Delta)\epsilon(\mathbf{k}) = (1+\Delta)J(0)(1-\gamma_k{}^2)^{1/2}. \quad (7.20)$$

This is precisely Oguchi's result.[3]

## 8. THE $1/z$ EXPANSION; CONCLUSIONS

Let us now recapitulate, taking stock of the results of our various diagram summations. In particular we wish to interpret the significance of our choice of diagrams and to establish the $1/z$ criterion which has been assumed implicitly in that choice.

Returning to the initial summation of simple chain diagrams (with neither locks nor longitudinal interactions) it will be recalled that we obtained the familiar Anderson spin-wave theory.[2] This is hardly surprising, for the Anderson theory is characterized by two approximations. Firstly, simple spin-wave theory replaces $S^+$ by $(2S)^{1/2}a$, and $S^-$ by $(2S)^{1/2}a^+$, where $a$, $a^+$ are boson operators, thereby ignoring the kinematical limitation to $2S+1$ states at each lattice point; a limitation represented by locks in our diagrams, and ignored in the chain approximation. Similarly the $S_i{}^zS_j{}^z$ terms in the Hamiltonian are replaced by $S^2-S(a_i{}^+a_i+a_j{}^+a_j)$, thereby neglecting the longitudinal interaction $a_i{}^+a_ia_j{}^+a_j$ precisely as in our chain approximation.

In our next approximation we introduced self-energy corrections containing either a single lock or a single longitudinal interaction, asserting that either of these corrections is of order $1/z$. In fact we found, by direct calculation, that the self-energy contributions so obtained are, typically $\Sigma_2 = -2\delta S_0{}^z$ or $\Sigma_2+\Sigma_4=\Delta$. We must therefore estimate the magnitude of $\Delta$ and of $\delta S_0{}^z$; in Appendix C we show that each of these quantities is of order $1/z$.

Consider now the renormalization of an unperturbed Green's-function line with a bubble $\Sigma_3$. The ratio of the Green's function with one bubble to the bare Green's function is

$$G^0(\omega)\Sigma_3G^0(\omega)/G^0(\omega) = \Sigma_3G^0(\omega) = -2\omega_0\delta S_0{}^z/(\omega-\omega_0), \quad (8.1)$$

and inserting the simple spin-wave frequency for $\omega$ (the first-order frequency $\epsilon^{(1)}(\mathbf{k})$ would do as well) and taking $2\delta S_0{}^z\sim 1/z$,

$$G^0(\omega)\Sigma_3G^0(\omega)/G^0(\omega) = 1/z[\omega_0/(\omega_0-\epsilon(\mathbf{k}))]. \quad (8.2)$$

Consequently the ratio of the dressing to the bare Green's function is of order $1/z$ if $\epsilon(\mathbf{k})\ll\omega_0$ (long wavelength). Thus our $1/z$ criterion is meaningful only if $\epsilon(\mathbf{k})$ is less than (approximately) $\omega_0/2$. This restricts our theory to wavelengths greater than roughly two interspin distances.

It is of some interest to note that it is only the bubble renormalization which restricts the theory to long wavelengths. For instance, the addition to a transverse interaction of a loop ($\Sigma_2$) and a longitudinal interaction ($\Sigma_4$) simply replaces $J(\mathbf{k})$ by $J(\mathbf{k})\Delta$ [Eq. (7.17)], and the ratio of the dressing to the bare interaction lines is $\Delta\sim 1/z$, independent of $\mathbf{k}$.

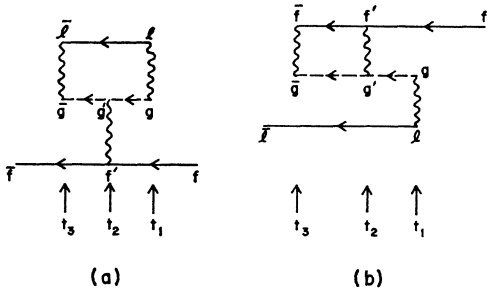


FIG. 10. Representative first-order correction diagrams.

The physical origin of the $1/z$ criterion now becomes evident. Consider first the bubble corrections and refer to diagram (a) of Fig. 10. The incoming Green's function line $G^0(\bar{f},f)$ represents a spin flipped up on the $f$ site (which is normally down), and precessing ("propagating") in the environment of its surrounding spins, all of which are presumed to be in the Néel ground-state configuration. However, in the true ground state there are vacuum fluctuations, one of which is shown to occur at time $t_1$ in the Figure. At that moment the normally up spin $g$ flips down and the normally down spin $l$ flips up (maintaining the total $S^z$, of course). This vacuum fluctuation occurs with a probability proportional to $\delta S_0{}^z$. There are, however, $z$ neighbors, so that the probability of such a flipped neighbor is of the order of unity. This situation is comparable to that in Fig. 10(b), in which the existence of the annihilation process at $t_3$ guarantees the existence of a flipped neighbor just prior to $t_3$. In both cases the correction diagram then depends on the probability that the longitudinal interaction will occur before the neighboring spin-flip annihilates. The vacuum fluctuations which occur at time $t$ have energy $\omega_0$, and by the uncertainty principle they have a mean lifetime $\langle t_3-t_1\rangle\sim 1/\omega_0$. The occurrence of a longitudinal interaction during this time is brought about by the operator $\exp(-iJ'S^+S^-R^+S^-t)$, so that we can consider such interactions to occur with a frequency of order $J'$. Thus the probability of an interaction in the interval $t_3-t_1$ is $J'\langle t_3-t_1\rangle\sim J'/\omega_0=1/z$.

If this heuristic argument does not seem plausible (and it is meant to be only that, rather than a proof, which has already been given) an alternative way to consider the probability of a longitudinal interaction is as follows. The amplitudes of longitudinal interaction and annihilation process are governed, respectively, by the matrix elements $J'(0|S^+S^-R^+R^-|0)$ and $J(0|S^-R^-|0)$. The ratio is $(0|S^+S^-R^+R^-|0)/(0|S^-R^-|0) \sim (\delta S_0{}^z)^2/\delta S_0{}^z\sim 1/z$.

We turn our attention now to the kinematical loop or lock diagrams. The purpose of these diagrams is to correct the error committed in the simple spin-wave (chain) theory, in which the spin states were approximated by boson states. Our single-lock diagram corrects

the first nonphysical state ($m=2$ for $S=\frac{1}{2}$; more generally the first nonphysical state would be $m=2S+1$). Now the probability of population of the various boson states *in the simple spin-wave theory* is exponential,[10,11] $P_m=e^{-am}/\sum_0^\infty e^{-am'}$. The parameter $a$ in this probability distribution can be related to the physical quantity $\delta S_0{}^z$, for

$$\delta S_0{}^z=\langle m\rangle=\sum me^{-am}/\sum e^{-am}=1/(e^a-1), \quad (8.3)$$

whence

$$P_2=e^{-2a}-e^{-3a}=\left[\frac{\delta S_0{}^z}{1+\delta S_0{}^z}\right]^2 -\left[\frac{\delta S_0{}^z}{1+\delta S_0{}^z}\right]^3\sim(\delta S_0{}^z)^2. \quad (8.4)$$

Higher order lock diagrams eliminate the third, fourth, etc. nonphysical states, with population probabilities $P_3\sim(\delta S_0{}^z)^3$, $P_4\sim(\delta S_0{}^z)^4$, etc. Again we observe the ordering of the kinematical correction diagrams in powers of $1/z$.

It is of interest to note the existence of a stringent internal test of self-consistency in our theory. The isotropy of the Hamiltonian precludes the presence of an energy gap in the excitation spectrum. Maintenance of this isotropy throughout the calculation requires a delicate balance of diagrams involving longitudinal interactions with those involving transverse interactions. Any arbitrary selection of diagrams has an overwhelming probability of upsetting this balance and giving an energy gap. The classification according to $1/z$ is strongly substantiated by its success in maintaining isotropy to the given order.

With the $1/z$ criterion thus rationalized we examine the result of the first order calculation. We found that, except for extremely short wavelength spin waves, the spin-wave energies are

$$\epsilon^{(1)}(\mathbf{k})=(1+\Delta)J(0)(1-\gamma_{\mathbf{k}}{}^2)^{1/2}=(1+\Delta)\epsilon(\mathbf{k}). \quad (8.5)$$

This result is identical to that found by Oguchi,[3] who ostensibly obtained the spectrum for all wavelengths. The Oguchi method is based on expansion of the Holstein-Primakoff radical

$$S_f{}^-=(2S)^{1/2}a^+(1-(a^+a/2S))^{1/2}=(2S)^{1/2} \times a^+[1-(a^+a/4S)-[(a^+a)^2/32S^2]-\cdots]. \quad (8.6)$$

This method appears to us to be of dubious validity for $S=\frac{1}{2}$. The magnitude of the $p$th term is $\sim\langle(a^+a)^p\rangle/S^p$. However, for an exponential probability distribution $\langle(a^+a)^p\rangle$ is of the order of $\langle a^+a\rangle$, independent of $p$ (for example one easily computes $\langle(a^+a)^2\rangle=\langle a^+a\rangle+2\langle a^+a\rangle^2$). Thus the numerators in the expansion (8.6) are all of the same order, and the expansion is strictly an expansion in $1/2S$.

Mattis,[12] in his recent book comments on the procedure of expansion of the square roots in the Holstein-Primakoff representation. "For large spins, the agreement of even the linearized theories with the classical equations of motion gives some confidence in this procedure, for which there is no other formal mathematical justification." The present authors confess surprise that, except for very short wavelength, we corroborate Oguchi's result.

## APPENDIX A: WICK'S THEOREM

A direct proof of Wick's theorem for spin operators is given below; a simple alternative proof using the coupled-fermion representation[12] of spin operators has been given elsewhere.[13]

To prove the form of Wick's theorem enunciated in Eq. (2.10) it is convenient to define the analog of the Wick time-ordering operator $T$. The $T$ product of a sequence of $S^+$ and $S^-$ operators arranges the factors in increasing time order from right to left, multiplying the product by $-1$ for each interchange of two spin operators *of the same site* necessary to achieve the chronological order. Again, if an $S^+$ and an $S^-$ operator have equal time arguments, the $S^+$ is ordered to the left.

We also define the symbols

$$\eta_{lm}=1-2\delta_{lm}\theta(t_m-t_l), \quad (A1)$$

where

$$\theta(t_m-t_l)=1, \text{ if } t_m>t_l; \quad =0, \text{ if } t_m\leqslant t_l; \quad (A2)$$

and, since products of the $\eta$'s frequently occur,

$$\eta(l_1,l_2,\cdots)\equiv\prod_{l_i<l_j}\eta_{l_il_j}. \quad (A3)$$

Then the relationship between the $P$ and $T$ products can be written conveniently in the form

$$\langle 0|PS_1{}^-(t_1)S_2{}^+(t_2)S_3{}^-(t_3)\cdots|0\rangle =\langle 0|TS_1{}^-(t_1)S_2{}^+(t_2)S_3{}^-(t_3)\cdots|0\rangle\eta(1,2,3,\cdots). \quad (A4)$$

In the special case in which $r_1=r_2=r_3\cdots$ the product $\eta(1,2,3,\cdots)=\eta_{12}\eta_{13}\cdots\eta_{23}\eta_{24}\cdots$, and each factor such as $\eta_{23}$ is simply $+1$ if $t_2>t_3$ and is $-1$ if $t_2<t_3$, exactly cancelling the minus signs introduced by the $T$ operator. In the more general case in which $r_1\neq r_2$, for instance $\eta_{12}=1$, and the entire product merely factors into products for individual sites, to each of which the discussion above again applies.

Consider a single subproduct, and suppress the common site index:

$$\langle 0|PS^-(t_1)S^+(t_2)S^-(t_3)\cdots|0\rangle =\langle 0|TS^-(t_1)S^+(t_2)S^-(t_3)\cdots|0\rangle\eta(1,2,3,\cdots). \quad (A5)$$

[10] H. B. Callen and S. Shtrikman, Solid State Commun. **3**, 5 (1965).

[11] J. Van Kranendonk and J. H. Van Vleck, Rev. Mod. Phys. **30**, 1 (1958).

[12] D. Mattis, *The Theory of Magnetism* (Harper and Row, New York, 1965), p. 171.

[13] Yung-Li Wang, S. Shtrikman, and Herbert Callen, J. Appl. Phys. **37**, 1451 (1966).

Since, for a single site, the commutation relations of the spin operators are identical to those of fermion operators, the Wick product on the right of Eq. (A5) is subject to Wick's theorem in its usual form:

$$\begin{aligned}\langle 0|PS^-(t_1)S^+(t_2)S^-(t_3)S^+(t_4)\cdots S^+(t_{2n})|0\rangle \\ =\{\langle 0|TS^-(t_1)S^+(t_2)|0\rangle\langle 0|TS^-(t_3)S^+(t_4)|0\rangle\cdots \\ \times\langle 0|TS^-(t_{2n-1})S^+(t_{2n})|0\rangle \\ \pm\langle 0|TS^-(t_1)S^+(t_4)|0\rangle\langle 0|TS^-(t_3)S^+(t_2)|0\rangle\cdots \\ \times\langle 0|TS^-(t_{2n-1})S^+(t_{2n})|0\rangle \\ \pm\cdots\}\eta(1,2,\cdots,2n). \quad \text{(A6)}\end{aligned}$$

It will be recalled that the sign of each term is determined by the number of interchanges required to rearrange the operators from their order in the left-hand member to the order in the particular term in the right-hand member.

There are, of course, various rearrangements of the operators in the left-hand member of Eq. (A6), and these must all give identical results. For instance we can rewrite Eq. (A6) with 1, 2, 3, $\cdots$ replaced by 1′, 2′, 3′, $\cdots$, where 1′, 3′, 5′, $\cdots$ is any permutation of 1, 3, 5, $\cdots$ and 2′, 4′, 6′ is any permutation[14] of 2, 4, 6, $\cdots$ and where, of course, $i$ and $j$ are replaced by $i'$, $j'$ in the factors $\eta_{ij}$. The first term in the new equation, or

$$\begin{aligned}\langle 0|TS^-(t_{1'})S^+(t_{2'})|0\rangle \\ \times\langle 0|TS^-(t_{3'})S^+(t_{4'})|0\rangle\cdots\eta(1',2',\cdots),\end{aligned}$$

must then be identical to one of the terms appearing in Eq. (A6), whence $\eta(1',2',\cdots)=\pm\eta(1,2,\cdots)$, the $\pm$ sign depending on the parity of the permutation from 1, 2, 3, $\cdots$ to 1′, 2′, 3′, $\cdots$. It follows that Eq. (A6) can be rewritten in the more symmetrical form

$$\begin{aligned}\langle 0|PS^-(t_1)S^+(t_2)S^-(t_3)\cdots|0\rangle \\ =\sum_{\{i'\}}\{\langle 0|TS^-(t_{1'})S^+(t_{2'})|0\rangle \\ \times\langle 0|TS^-(t_{3'})S^+(t_{4'})|0\rangle\cdots\eta(1',2',\cdots)\}, \quad \text{(A7)}\end{aligned}$$

where the summation is over every permutation of 1, 3, 5, $\cdots$ to 1′, 3′, 5′, $\cdots$, and of 2, 4, 6, $\cdots$ to 2′, 4′, 6′, $\cdots$. Furthermore, we note that

$$\langle 0|TS^-(t_{1'})S^+(t_{2'})|0\rangle=iG^0(t_{1'},t_{2'}), \quad \text{(A8)}$$

as can be corroborated by noting that the $P$ and $T$ products are equal if $t_{1'}>t_{2'}$, whereas both sides of Eq. (A8) vanish if $t_{1'}\leq t_{2'}$. Finally we obtain

$$\begin{aligned}\langle 0|PS^-(t_1)S^+(t_2)S^-(t_3)\cdots|0\rangle \\ =\sum\{iG^0(t_{1'},t_{2'})iG^0(t_{3'},t_{4'})\cdots\eta(1',2',\cdots)\}. \quad \text{(A9)}\end{aligned}$$

Of the various $\eta_{i'j'}$ factors occurring in $(1',2',\cdots)$, those with subscripts corresponding to a single Green's function are redundant. This results from the fact that $G^0(t_{i'},t_{j'})=0$ if $t_{i'}<t_{j'}$, whereas $\eta_{i'j'}=1$ if $t_{i'}>t_{j'}$.

[14] Other permutations, which intermix even and odd indices, lead to Green's functions like $\langle 0|TS^-(t_1)S^-(t_3)|0\rangle$, which vanish.

The pictorial representation discussed in Sec. 2, and indicated in Fig. 1, provides a useful interpretation of the quantity $\eta(1,2,\cdots)$. For the $f$ site, the first set of contractions in Fig. 1 contains the nonredundant factors $\eta_{65}\eta_{64}\eta_{52}\eta_{42}=(+1)^4=1$, whereas the second set of contractions contains the nonredundant factors $\eta_{65}\eta_{62}\eta_{45}\eta_{42}=(+1)(+1)(-1)(+1)=-1$. The Green's functions in the first case are totally overlapping, and those in the second case are half-overlapping. A moment's reflection reveals that *the product of $\eta_{ij}$ factors is positive for non-overlapping or totally overlapping pairs of Green's functions, and is negative for half-overlapping pairs of Green's functions.*

For more than four operators the average value $\langle 0|PS^-(t_1)S^+(t_2)\cdots S^+(t_{2n})|0\rangle$ is again the sum of product of Green's functions corresponding to all possible contractions. Each product carries the signature $(-1)^Q$, where $Q$ is the number of pairs of half-overlapping Green's functions.

The discussion above was restricted to products of operators corresponding to a single site. In fact the result can be written without this restriction, for the "extra" permutations (which pair operators of different sites) vanish by virtue of the delta function in the unperturbed Green's functions [cf., Eq. (2.8)]. Consequently, we write the more general form of Wick's theorem for spin operators as

$$\begin{aligned}\langle 0|PS_f^-(t_f)S_g^+(t_g)S_l^-(t_l)S_m^+(t_m)\cdots|0\rangle \\ =\sum_{\{\alpha\}}\{iG_{\alpha\beta}{}^0iG_{\gamma\delta}\cdots\eta(\alpha,\beta,\gamma,\delta,\cdots)\} \\ =\sum_{\{\alpha\}}\{iG_{\alpha\beta}{}^0iG_{\gamma\delta}\cdots(-1)^Q\}, \quad \text{(A10)}\end{aligned}$$

where $\alpha,\beta,\gamma,\cdots$ is a permutation of $f, g, l, \cdots$ and $Q$ is the number of half-overlapping pairs of Green's functions (i.e., pairs of Green's functions with the same spatial indices and half-overlapping time indices).

## APPENDIX B: THE SYMMETRY FACTOR

The origin of the symmetry factor is the $1/(n!)$ factor appearing in the $n$th term of the expansion of $\mathcal{S}(t)$. It will be recalled that this factor was precisely cancelled by the multiplicity of the diagrams (under permutation of indices) in the ferromagnet. Because of the occurrence of disconnected diagrams this cancellation no longer follows. We must therefore turn our attention to the recurrent problem of diagram counting.

By convention the set of diagrams representing the numerator of the Green's function $G(\bar{l},m)$ contains only a single diagram of a given structure (two diagrams are said to have the same structure if they can be deformed into each other, ignoring differences in labelling indices). To each such diagram we must associate a multiplicity factor describing the number of terms (in the algebraic expansion) corresponding to this structure. For definiteness, consider a particular diagram with $m$ of each of

the two kinds of transverse interactions and $n'=n-2m$ longitudinal interactions. This arises from a product of $n$ factors $\mathcal{H}_1\mathcal{H}_1\cdots\mathcal{H}_1$ in the expansion of $\mathcal{S}(\infty)$. The particular diagram, which attributes the $n'$ longitudinal interactions to a particular set of $n'$ ion pairs, is achieved many ways in the product $\mathcal{H}_1\mathcal{H}_1\cdots\mathcal{H}_1$; the longitudinal part of $\mathcal{H}_1$ can be chosen from $n'$ of these $n$ factors in $\binom{n}{n'}$ ways, and then the site labels can be distributed in $n'!$ ways among these $n'$ factors. Thus the longitudinal interactions contribute a multiplicity of

$$n'!\binom{n}{n'}=\frac{n!}{(n-n')!}=\frac{n!}{(2m)!}.$$

Similarly one type of transverse interaction can now be chosen in

$$\binom{n-n'}{m}$$

ways from the remaining $(n-n')$ factors of $\mathcal{H}_1$, and then the site labels can be distributed in $m!$ ways. Finally, the remaining transverse interactions permit only a permutation of the site labels in $m!$ ways. Collecting these factors, we have a multiplicity of

$$\frac{n!}{(2m)!}\frac{(2m)!}{(m!)^2}(m!)^2=n!$$

exactly cancelling the expansion factor $1/n!$, precisely as in the ferromagnetic case. However, we now recognize that the internal indices are to be summed over. For a disjoint portion of a diagram this summation can reproduce some of the terms which have already been counted in the multiplicity factor $n!$. Thus in the diagram of Fig. 3(d) the same term will be achieved when $f_1=1$, $f_2=2$, $g_1=3$, $g_2=4$ as when $f_1=2$, $f_2=1$, $g_1=4$, $g_2=3$. Thus the summation over indices overcounts diagrams. We therefore define a symmetry factor $\gamma$ [$=2$ in the case of Fig. 3(d)] which is the order of the symmetry group of the diagram, or the number of ways in which the (unlabelled) diagram can be rotated into itself. The contribution of each diagram must then be divided by the appropriate symmetry factor $\gamma$.

## APPENDIX C: MAGNITUDES OF $\delta S_0{}^z$ AND OF $\Delta$

The clue to the magnitude of $\delta S_0{}^z$ and of $\Delta$ lies in the easily proved identity

$$\langle\gamma^2\rangle\equiv\frac{1}{N}\sum_{\mathbf{k}}\gamma_{\mathbf{k}}{}^2=\frac{1}{z}, \tag{C1}$$

which holds for systems with nearest-neighbor interactions and with a center of reflection symmetry at each magnetic ion. Expanding the radical in Eq. (7.5) we find

$$\delta S_0{}^z=\tfrac{1}{2}\{\tfrac{1}{2}\langle\gamma^2\rangle+\tfrac{3}{8}\langle\gamma^4\rangle+\tfrac{5}{16}\langle\gamma^6\rangle+\cdots\}. \tag{C2}$$

The ratio of terms can be computed for simple structures

$$\begin{aligned}&\langle\gamma^4\rangle/\langle\gamma^2\rangle=0.42\ (\text{sc}),\quad 0.42\ (\text{bcc})\\&\langle\gamma^6\rangle/\langle\gamma^2\rangle=0.24\ (\text{sc}),\quad 0.24\ (\text{bcc})\\&\langle\gamma^8\rangle/\langle\gamma^2\rangle=0.15\ (\text{sc}),\quad 0.16\ (\text{bcc})\end{aligned} \tag{C3}$$

suggesting that $\langle\gamma^{2n}\rangle/\langle\gamma^2\rangle=2^{-n+1}$ as a rough approximation. This approximation would give [re-summing the series (C2)]

$$\delta S_0{}^z\sim(1/z)\{[1/(1-\tfrac{1}{2})^{1/2}]-1\}\sim(1/2z). \tag{C4}$$

In fact $\delta S_0{}^z$ has been calculated for several structures[15,16] and it appears to lie between $1/4z$ and $1/2z$; for simple cubic $\delta S_0{}^z=0.078$ whereas $1/2z=0.083$; for bcc $\delta S_0{}^z=0.059$ whereas $1/2z=0.062$. Thus *we henceforth consider $2\delta S_0{}^z$ to be of order $1/z$, and similarly for the closely related quantity $\Delta$.*

[15] R. Kubo, Phys. Rev. 87, 568 (1952).
[16] H. C. Davis, J. Phys. Chem. Solids 23, 1348 (1962).